lubricants

MDPI

Article

Boric Acid as an Effective Lubricant Additive in Glycerol Ethoxylate Aqueous Solution

Shouzhi Huang [1], Zhongnan Wang [2,*] and Zhongxian Hao [1]

[1] Research Institute of Petroleum Exploration & Development (RIPED), PetroChina, Beijing 100083, China; huangsz1@petrochina.com.cn (S.H.); haozx@petrochina.com.cn (Z.H.)
[2] School of Mechanical, Electronic and Control Engineering, Beijing Jiaotong University, Beijing 100044, China
* Correspondence: zhn.wang@bjtu.edu.cn

Abstract

Global temperature increases and more frequent extreme climate events have intensified the challenges faced by oil-based lubricants, including environmental impact and resource depletion. In recent years, glycerol ethoxylate (GE), a non-toxic and low-cost compound, has shown promise as a water-based lubricants capable of replacing conventional oil-based systems. Boric acid (BA) is an effective additive that significantly improves the extreme pressure performance of water-based lubricants. This study demonstrates that adding BA to a GE aqueous solution decreases the friction coefficient by five times and increases extreme pressure by 12.5%. Higher concentrations of BA promote the formation of a lubricating film, enhancing the hydrodynamic pressure effect. The findings provide valuable insights into the formulation and tribological behavior of eco-friendly lubricants, promoting sustainable manufacturing, longer equipment life, and improved reliability.

Keywords: glycerol ethoxylate; boric acid; water-based lubricant; friction and wear; film-forming behaviour

check for updates

Received: 21 August 2025
Revised: 11 September 2025
Accepted: 12 September 2025
Published: 16 September 2025

Citation: Huang, S.; Wang, Z.; Hao, Z. Boric Acid as an Effective Lubricant Additive in Glycerol Ethoxylate Aqueous Solution. *Lubricants* **2025**, *13*, 414. https://doi.org/10.3390/lubricants13090414

Copyright: © 2025 by the authors. Licensee MDPI, Basel, Switzerland. This article is an open access article distributed under the terms and conditions of the Creative Commons Attribution (CC BY) license (https://creativecommons.org/licenses/by/4.0/).

1. Introductions

Mechanical components are subject to surface degradation due to various forms of wear during friction, often leading to equipment failure. Traditionally, oil-based lubricants have been applied in the industry to mitigate these effects, but their continued use contributes to environmental pollution [1]. Water-based lubricants have gained interest in metalworking, coolant applications, and hydraulic systems, due to their biodegradability and excellent tribological performance [2]. Despite these advantages, they typically suffer from lower adhesion pressure and surface tension, resulting in reduced film-forming capacity and corrosion resistance compared to oil-based lubricants.

Recent studies [3] have shown that introducing functional additives into water-based lubricants can produce synergistic effects that enhance tribological performance, film-forming, and corrosion resistance, sometimes even surpassing their oil-based counterparts. Functional water-based lubrication additives span a range of materials, including sulfur- and phosphorus-based compounds, boron-containing species, nanoparticles [4], and water-soluble polymers [5].

Sulfur and phosphorus react with friction surfaces to form boundary films, significantly improving wear resistance. For example, Xiong [6] developed a water-soluble additive containing sulfur and phosphorus. These additive forms tungsten-based boundary films during operation, enhancing the lubricant's extreme pressure tolerance by five

times. However, the waste generated from these additives is frequently toxic and harmful to the environment.

Boron-based additives, including nano-metal borates, have shown improved lubrication and pressure resistance by forming protective films. Saffari's research [7] on magnesium, zinc, aluminum, and titanium borates demonstrated significant improvements in drilling fluid performance. Xie [8] discovered that carbon nanotube (CNT)-SiO_2 composite nanofluids offer superior load capacity and lubrication film stability, reducing the friction coefficient and wear rate by 30.6% and 34.1%, respectively, compared to CNT or SiO_2 nanofluids alone.

Water-soluble polymers typically contain hydrophilic groups (such as carboxyl, amino, and hydroxyl groups), which offer excellent film-forming ability, dispersion stability, and superior anti-friction and anti-wear properties [9,10]. Fernando's research [11] on green additives using alkyl glycerol ether and xanthan gum resulted in strong adsorption films, with tribological performance improving as the alkyl chain length increased. Despite these advancements, a performance gap still exists under high-temperature and high-load conditions. Thus, further research is needed to explore the compatibility and synergistic effects of combined lubricant additives to optimize the anti-friction, wear-resistance, film-forming, and anti-corrosion properties of water-based lubricants.

Glycerol ethoxylate (GE) is a non-ionic surfactant known for its excellent dispersion, stability, wettability, solubilization, and compatibility with other lubricants [12,13]. Meng's previous research [14] demonstrated a link between the molecular weight of GE and the friction coefficient, indicating that higher molecular weight enhances adsorption and load-bearing capacity due to the presence of ether groups. Boric acid (BA), as a weak acid, is commonly used as a lubricant additive because of its excellent lubrication properties [15] and environmental compatibility [16]. As a hydrate of boric oxide (B_2O_3), thin films from borates have low shear strength, allowing smooth sliding between contact surfaces and lowering the friction coefficient. This is attributed to the presence of hydrogen bonds [16].

In this study, BA was used as a water-based lubrication additive in GE aqueous solution to evaluate its tribological performance. The physicochemical interactions between BA and GE in a mixed solution were systematically examined, with emphasis on rheological behavior and surface wettability. Comprehensive tribological assessments were conducted to evaluate anti-friction and anti-wear characteristics under varying conditions, both pre- and post-friction testing. The extreme pressure tolerance and anti-corrosion properties of the BA–GE formulation were further analyzed. Film-forming behaviour on contact surfaces was further characterized to elucidate the underlying lubrication mechanisms. These findings provide essential insights toward the rational design of high-performance, environmentally sustainable water-based lubricants for industrial applications.

2. Experiments

2.1. Lubricant and Additive

Glycerol ethoxylate (GE, 99.5%, Jiangsu Huai'an Petrochemical Plant, Huai'an, China) and boric acid (BA, 99.8%, Sino-phosphoric Chemical Reagent Co., Ltd., Shanghai, China) were used as water-based lubricant additives. GE-26 with high molecular weight (1236, $HO(CH_2CH_2O)_nCH[CH_2(OCH_2CH_2)_nOH]_2$) has a long carbon chain that contains ether groups, to provide excellent adsorption force and bearing capacity [14].

While BA has been studied for its tribological benefits (e.g., as a solid lubricant or additive due to its layered structure and shear properties), its acidic nature may pose corrosion risks, particularly in the presence of water or at high temperatures. However, BA could improve the mechanical properties and heat resistance and offer extreme pressure

capacity as an auxiliary additive due to the presence of boron, for various applications such as medical treatment and aerospace fields [17–19].

To prepare the lubricating reagents, first use an electronic balance to weigh the required amounts of GE26 and BA. Then, use a burette to add the required volume of deionized water to a beaker. Stir the mixture with a glass rod for 3 min to dissolve the solute, followed by 20 min of stirring with a magnetic stirrer to ensure complete dissolution. Finally, let the solution stand for 30 min before use.

Aqueous GE solutions of varying concentrations (1%, 5%, 10%, 15%, 20 wt%, 30 wt%, 40 wt%, 50 wt%, 60 wt% and 70 wt%) were prepared using deionized water, which were labeled as 1%GE, 5%GE, 10%GE and so on, respectively. However, GE solutions with concentrations of 1%, 5%, 10%, and 15% all caused significant abnormal noise during the four-ball friction tests, making it impossible to continue the experiment. Meanwhile, BA-50%GE mixed solutions were initially prepared in various ratios (1:3, 1:5, 1:10, 1:15, 1:20, 1:25), which were labeled as BA-50%GE-(1:3), BA-50%GE-(1:5), BA-50%GE-(1:10) and so on, respectively. However, precipitates were observed in the solutions with ratios of 1:3 and 1:5 after long-term standing. This is primarily due to the high boron acid content, which causes the solution to reach saturation, preventing it from dissolving completely. Thus, tribological studies were carried out on GE using concentrations of 20%, 30%, 40%, 50%, 60% and 70%, as well as mixed solutions with ratios of 1:10, 1:15, 1:20, and 1:25.

All the ratios of BA-GE mixed solutions were weight/weight. It is noteworthy that a small number of bubbles appeared in GE aqueous solution following stirring, with the number and intensity of bubbles increasing proportionally with concentration. However, an obvious reduction in bubble density was recorded upon the introduction of BA, indicating its capacity to suppress foaming and enhance solution stability.

2.2. Equipment and Methods

(1) Friction properties

The tribological performance of GE aqueous solution and BA-GE mixed solution were studied using a four-ball friction and wear tester (SGW-10A, Jinan Hengxu Testing Machine Technology Co., Ltd., Jinan, China). GCr15 bearing steel balls (12.7 mm diameter) served as friction pairs. Prior to the tests, the steel balls were ultrasonically cleaned in petroleum ether and anhydrous ethanol for 15 min, rinsed with deionized water, and subsequently dried. The applied normal load ranges from 100 N to 500 N, corresponding to the maximum contact pressure of approximately 750 MPa via Hertzian contact theory, and the linear velocity varies from 600 mm/s to 1200 mm/s. Each test was conducted three times to minimize errors from accidental factors. All the tests were conducted at a temperature of 25 °C and a relative humidity of 30 ± 5%. The solutions before and after the friction experiments were compared to study the effect of BA on the anti-corrosion property of GE aqueous solutions.

A three-dimensional (3D) white-light interference surface topography instrument (Nexview NX2, 3D Optical Profilers, ZYGO, Middlefield, CT, USA) was used to measure the diameter of the wear scar on the surfaces of three steel balls for the investigation of the anti-friction and anti-wear effect of the water-based lubricant. The wear surface of the steel balls was also measured using X-ray photoelectron spectrometer (ESCALAB Xi+ XPS, ThermoFisher Scientific, Shanghai, China) with the depth of less than 10 nm, and the detection limit of elements of 0.01–1 at% at room temperature. The chemical composition and reactions at the wear surface were analyzed to investigate the chemical characteristics of the friction film before and after the introduction of BA.

(2) Lubricant characterizations

Fourier transform infrared (FT-IR) spectroscopy (Perkin Elmer, Instruments Co., Ltd., Shanghai, China) and Raman spectroscopy (LabRAM HR, HORIBA, Paris, France) were used to analyze the molecular structure, chemical bond, and composition variations in the lubricants before and after the addition of BA. Rheological properties were measured using a rotating rheometer (Physica MCR301, Aaton Paar, Graz, Austria), with shear rate logarithmically varied from 1 s^{-1} and 2000 s^{-1} and temperatures set at 25 °C, 50 °C, 75 °C and 90 °C, respectively. These rheological profiles indicate temperature-dependent viscosity and flow behavior, which directly affect the thickness and shape of the lubrication film during the friction process. The contact angle was measured using a video optical goniometer (OCA15EC, Dataphysics, Stuttgart, Germany), where 5 μL droplets of lubricant were deposited on steel surfaces and imaged after 5 s of stabilization at room temperature. Measurements were performed for pure water, GE aqueous solution of varying concentration, and BA-50%GE mixtures solution at different BA ratios, with each measurement repeated three times. The adsorption film, governed by the adhesion energy of lubricant molecules, is closely related to surface wetting behavior, which in turn influences the tribological properties of the lubricant on solid surfaces [20–22].

(3) Film-forming performance

To assess the lubricant's ability to form an effective tribological film on the friction surface, its film-forming properties were systematically evaluated [23–25]. The influence of characteristic length scales on lubrication behavior was analyzed via numerical solutions to the Reynolds equation for film lubrication [26]. The correlation between film-forming and anti-friction or anti-wear performance is generally limited, but the increase in film thickness is known to enhance the loading capacity of lubricants. The effects of linear velocity and lubricant concentration on the film-forming properties of GE aqueous solution and BA-GE mixed solutions were investigated using a photo-elasto-hydrodynamic lubrication film thickness measuring instrument [26].

(4) Extreme pressure performance

Given the inherently low load-bearing capacity of the water-based lubricants, the extreme pressure (EP) performance was evaluated by determining the maximum non-seizure load (P_B value). Testing was conducted at 25 °C with a sliding speed of 1760 rpm, under stepwise increasing loads of 314 N, 392 N, 490 N, and 618 N. Each test lasted 10 s, and the transition from mild to severe wear was identified by comparing the average wear scar diameters on the surface of the steel ball with the compensation diameter D_b of 1.05 times.

3. Results and Discussion

3.1. FT-IR and Raman

Figure 1a gives the FT-IR spectrum of the 50% GE aqueous solution. Two prominent absorption bands were observed at 3380.49 cm^{-1} corresponding to the O–H stretching vibration [27] and at 1642.93 cm^{-1}, attributed to H–O–H bending vibrations in water [28], potentially overlapping with unsaturated carbon contributions. These signals originate from the abundant hydroxyl groups in both pure water and GE molecules [29]. Characteristic absorption bands were observed at 1457.87 cm^{-1} (alkyl C–H bending), 1082.95 cm^{-1} (C–O stretching of secondary alcohols), and within the 650–1000 cm^{-1} range, possibly related to out-of-plane bending of C–H groups or ether ring vibrations [30]. Upon incorporation of BA, no significant changes in the spectral features were observed (Figure 1b), suggesting the absence of new covalent bond formation between GE and BA.

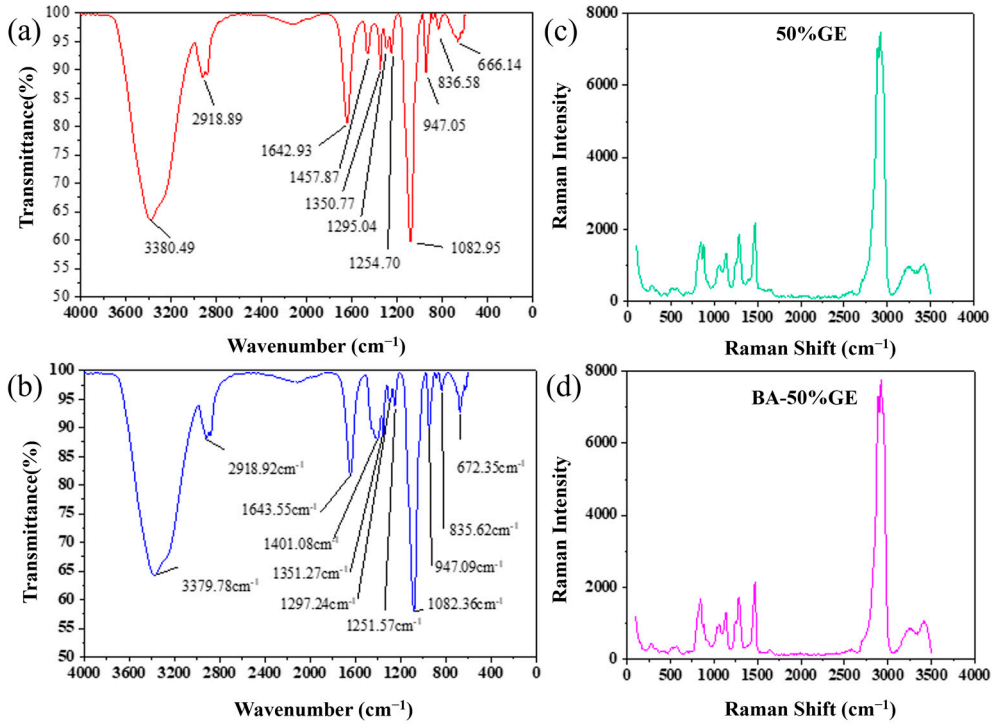


Figure 1. Infrared spectra of (**a**) 50%GE and (**b**) BA-50%GE mixed solutions, and Raman spectra of (**c**) 50%GE and (**d**) BA-50%GE mixed solutions.

The Raman spectrum of the 50%GE aqueous solution (Figure 1c) shows an O–H stretching band at 3409.73 cm^{-1}, primarily attributed to the hydroxyl groups in pure water and GE molecules [29]. Distinct peaks observed at 1282.34 cm^{-1} and 2919.41 cm^{-1} correspond to alkane C–H stretching modes [31], while those at 845.25 cm^{-1} and 1135.34 cm^{-1} are assigned to olefinic C–H vibrations. These features, alongside signals associated with C–O, C–C, $–CH_2–$, and –C=C– bonds, reflect the vibrational modes of the GE molecule. Notably, the Raman spectrum of the BA–GE mixed solution (Figure 1d) shows no new peaks or significant spectral shifts, indicating the absence of chemical bonding and suggesting that the interaction between BA and GE is predominantly physical in nature.

3.2. Rheological and Wettability Properties

The rheological behavior of 50%GE and BA-50%GE-(1:25) mixed solution was evaluated across a range of temperatures. Both systems exhibited a good linear increase in shear stress with shear rate (Figure 2a,b), indicative of Newtonian fluid behavior. For 50%GE (Figure 2c), the dynamic viscosity decreased markedly with increasing temperature, falling from ~22.5 mPa·s at 25 °C to 7.47 mPa·s at 75 °C. The variation range of the dynamic viscosity is about 10 mPa·s when the temperature increases from 25 °C to 50 °C, but there is only a little variation with a range of 0.25 mPa·s at higher temperatures of 75 °C and 90 °C. This phenomenon might be attributed to the rising temperature will increase the intermolecular distance and reduce the intermolecular force of the solute, leading to a decrease in solution viscosity [32]. A similar trend was observed in the BA-containing system (Figure 2d), with viscosity dropping from ~25 mPa·s at 25 °C to 6 mPa·s at 90 °C. Notably, the BA-containing system exhibited a smoother viscosity–temperature profile, suggesting enhanced thermal stability of the solution's rheological behavior. This behavior indicates that BA influences the microstructural arrangement of the GE matrix, possibly by altering intermolecular interactions or reducing the turbidity point.

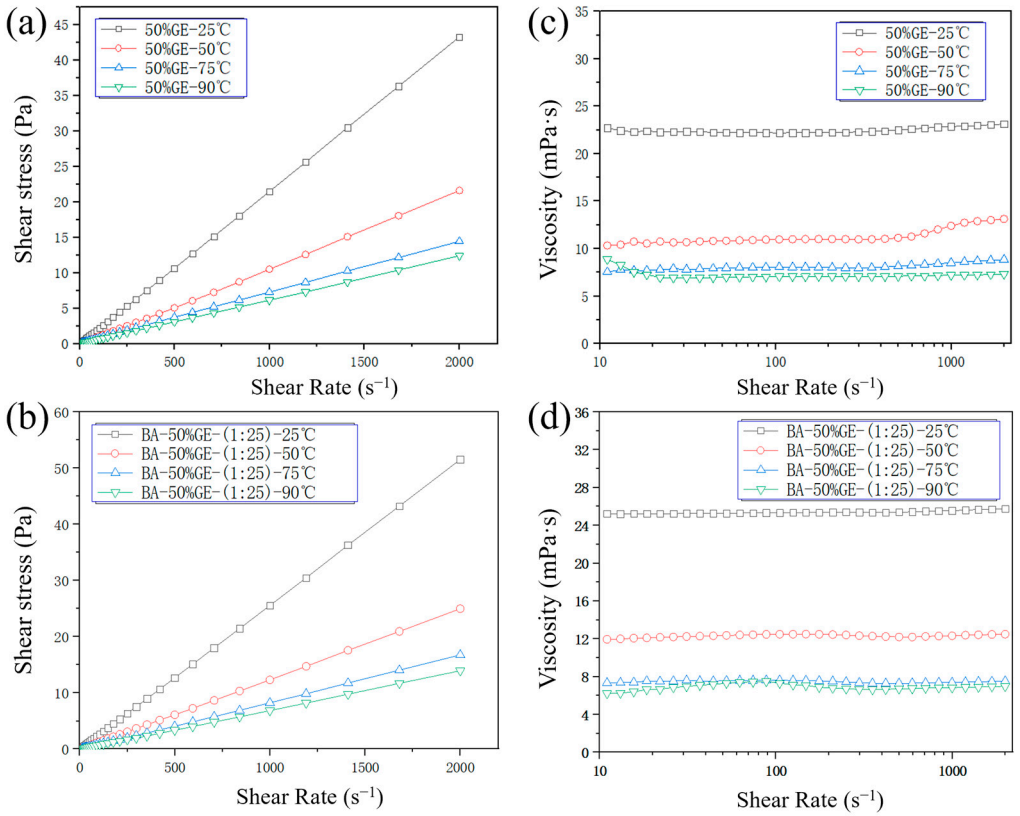


Figure 2. The relationship between shear stress and shear rate of (**a**) 50%GE aqueous solution and (**b**) BA-50%GE-(1:25) aqueous solution at different temperatures; the variations in dynamic viscosity of (**c**) 50%GE solution and (**d**) BA-50%GE-(1:25) aqueous solution with shear rate at different temperatures. Contact angle measurements were performed to evaluate the wettability of pure water, GE aqueous solution at varying concentrations, and BA-50%GE mixtures with different ratios (Figure 3). The contact angle of GE aqueous solutions remained below 60°, regardless of the BA addition. However, increasing the concentration of GE influenced the adhesive force and surface wettability, likely due to enhanced molecular adsorption on the steel surface. Upon incorporation of boric acid, the contact angle of all mixed solutions was smaller than that of a 50%GE aqueous solution, indicating that BA enhances the wettability of the GE solution, possibly by modifying surface tension or improving molecular alignment at the interface.

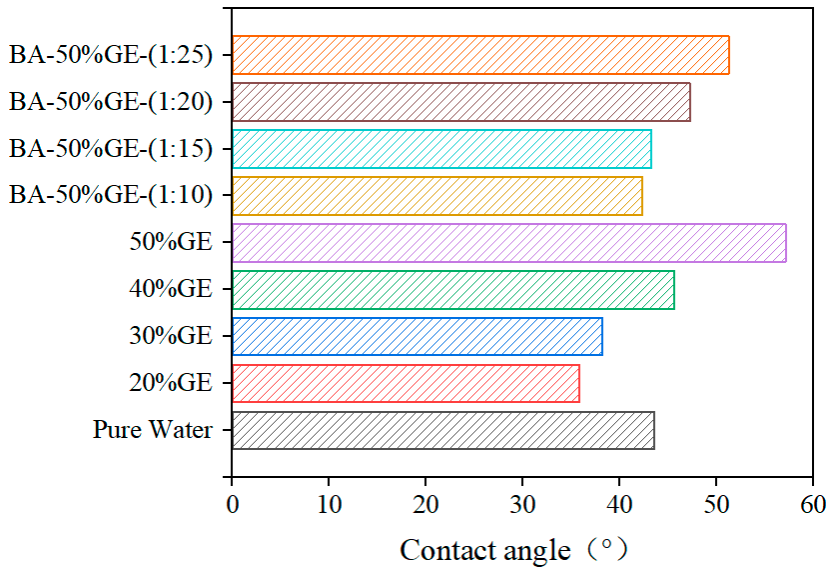


Figure 3. Variations in contact angle measurement for pure water and various lubricant additives.

3.3. Friction and Wear Properties

The friction coefficient of the GE aqueous solution was strongly influenced by its concentration (Figure 4a). At low concentrations (20% and 30%), the friction coefficient exhibited significant fluctuations, likely due to insufficient surfactant adsorption on the contact surfaces. As the concentration increased to 50%, the friction coefficient stabilized and decreased, indicating more effective film formation and enhanced lubrication. At concentrations above 50%, the friction coefficient began to increase again but gradually tend to stable.

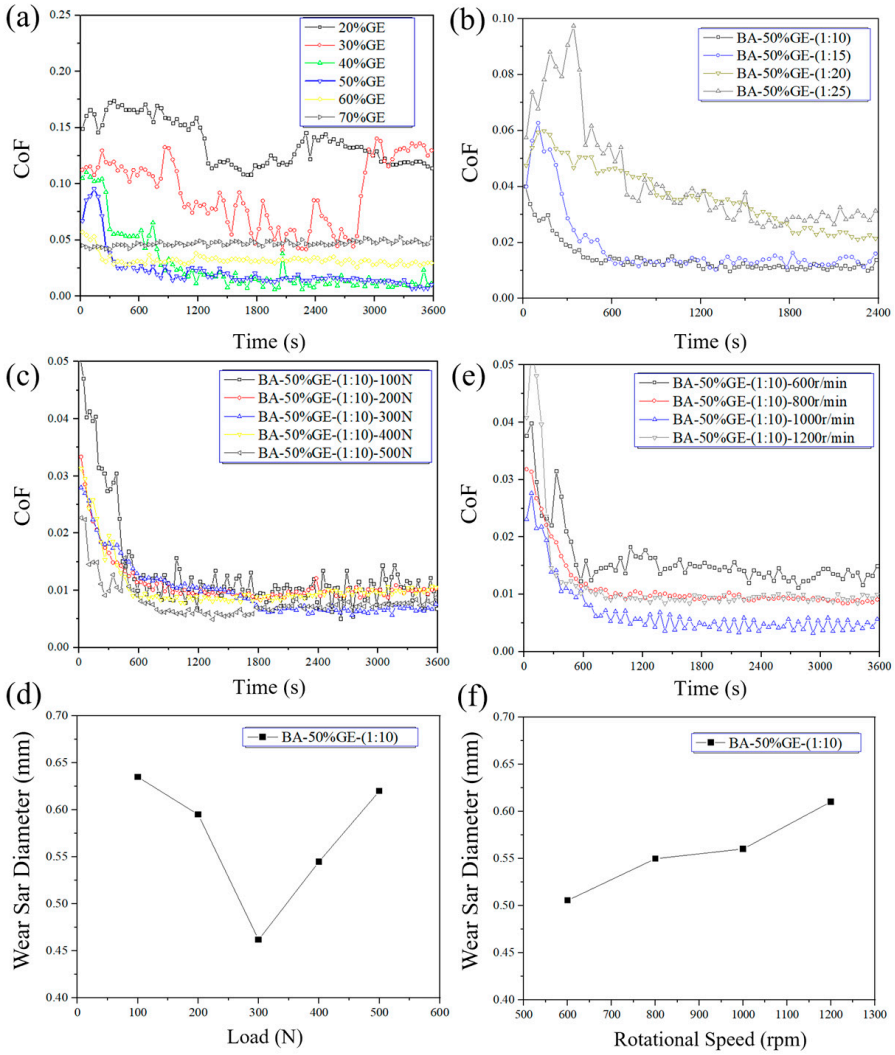


Figure 4. Variations in friction coefficient of (**a**) GE aqueous solution with different concentrations and (**b**) BA-50%GE mixed solution with different proportions; Variations in (**c**) friction coefficient and (**d**) wear diameter of BA-50%GE-(1:10) mixed solutions under various loads; Variations in (**e**) friction coefficient and (**f**) wear diameter of BA-50%GE-(1:10) mixed solution at different rotational speeds.

GE molecules are nonionic polyether compounds. Their hydrophilic polyethylene oxide chains extend into the aqueous phase, forming a dense adsorptive boundary lubricating film to replace direct 'metal-metal' contact. As the concentration increases, the solution viscosity rises due to the entanglement of the polyether chains. The contact area is in a mixed lubrication state, involving both boundary lubrication and a pressure film formed by the viscous fluid during the relative motion of the friction pair. This further supports the load, reduces contact, and lowers the friction coefficient. However, when GE concentration exceeds 50%, the solution viscosity increases exponentially. This can prevent the lubricating film from flowing and replenishing in time, forming a 'rigid adherent layer'

that increases friction. Moreover, the hydrogen bonding and hydrophobic association between GE molecules significantly enhance at high concentrations, forming 'molecular aggregates' that disrupt the boundary lubricating film, causing the friction coefficient to rise [14].

Nevertheless, the 50%GE solution was still chosen for further investigation due to its optimal solubility and minimal bubbles. GE aqueous solutions are more effective in forming a lubricating film between friction pairs at medium concentrations. Lower concentrations of GE aqueous solution result in fewer surfactant molecules being adsorbed on the friction surface, leading to a higher and more fluctuating friction coefficient [23].

Figure 4b illustrates that the friction coefficient for the BA-50%GE mixed solution at ratios of 1:10 and 1:15 showed minimal fluctuations, staying between 0.011 and 0.013. As the BA proportion decreases, the friction coefficient rises to 0.037 with significant fluctuations. This phenomenon is attributed to the initial lubricating film formed at lower BA concentrations being weaker. With higher BA content, chemical interactions between BA molecules and the friction surface promote the formation of a stronger lubricating film, thereby lowering the friction coefficient [33].

Figure 4c,d illustrate the effect of load on the friction coefficient and wear resistance of the BA-50%GE-(1:10) mixed solution at a sliding speed of 1000 rpm. The friction coefficient for the BA-50%GE mixture ranges from approximately 0.006 to 0.015, lower than that of the GE aqueous solution (0.05). As the load increases from 100 N to 300 N, the friction coefficient drops from 0.0135 to 0.0062 before stabilizing. When the load rises from 300 N to 500 N, the friction coefficient gradually increases with significant fluctuations.

The wear diameter changes correspondingly with the friction coefficient, reaching a minimum of 0.462 mm at a load of 300 N (Figure 4d). Thus, while the GE aqueous solution offers some anti-friction benefits, adding BA can further reduce the friction coefficient. The mixed solution performs well under lower loads, but under higher loads, the thin film formed by the water-based lubricant allows rough surface peaks to make direct contact, increasing friction and wear [34].

Figure 4e,f illustrate the changes in friction coefficient and wear resistance of the BA-50%GE-(1:10) mixed solution as the sliding speed increases from 600 rpm to 1200 rpm. The friction coefficient decreases to its lowest point (0.005) at 1000 rpm, then rises with further speed increases. The wear diameter also increases with speed, but only slightly, from 0.508 mm to 0.612 mm, indicating that the mixed solution performs best at 1000 rpm in terms of friction resistance. Additionally, the mixed solution shows a clear reduction in friction coefficient compared to the GE aqueous solution after adding BA.

The contact rate between rough peaks on the steel ball's surface increases with sliding speed, leading to higher wear rates and larger wear diameters [1]. Additionally, higher sliding speeds generate more friction heat and raise the aqueous solution temperature, reducing viscosity and anti-wear capability. Based on this analysis, the BA-50%GE-(1:10) mixed solution demonstrates the best anti-friction and anti-wear performance at 300 N and 1000 rpm.

3.4. XPS Energy Spectrum

Figure 5a indicates that the primary chemical elements detected on the worn surface of steel balls, when using GE aqueous solution as a lubricant, were carbon (C), oxygen (O), and iron (Fe). The electron binding energies for carbon were measured at 283.40 eV, 284.80 eV, 286.30 eV, and 288.30 eV, corresponding to the molecular structures $(–CH_2CH_2–)_n$, $(–CH_2CH_2O–)_n$, $(–CH_2CH(OH)–)$, and $(–(CH_2CH_2O)CH(CH_2OCH_2CH_2)_2–)_n$, respectively (Figure 5b).

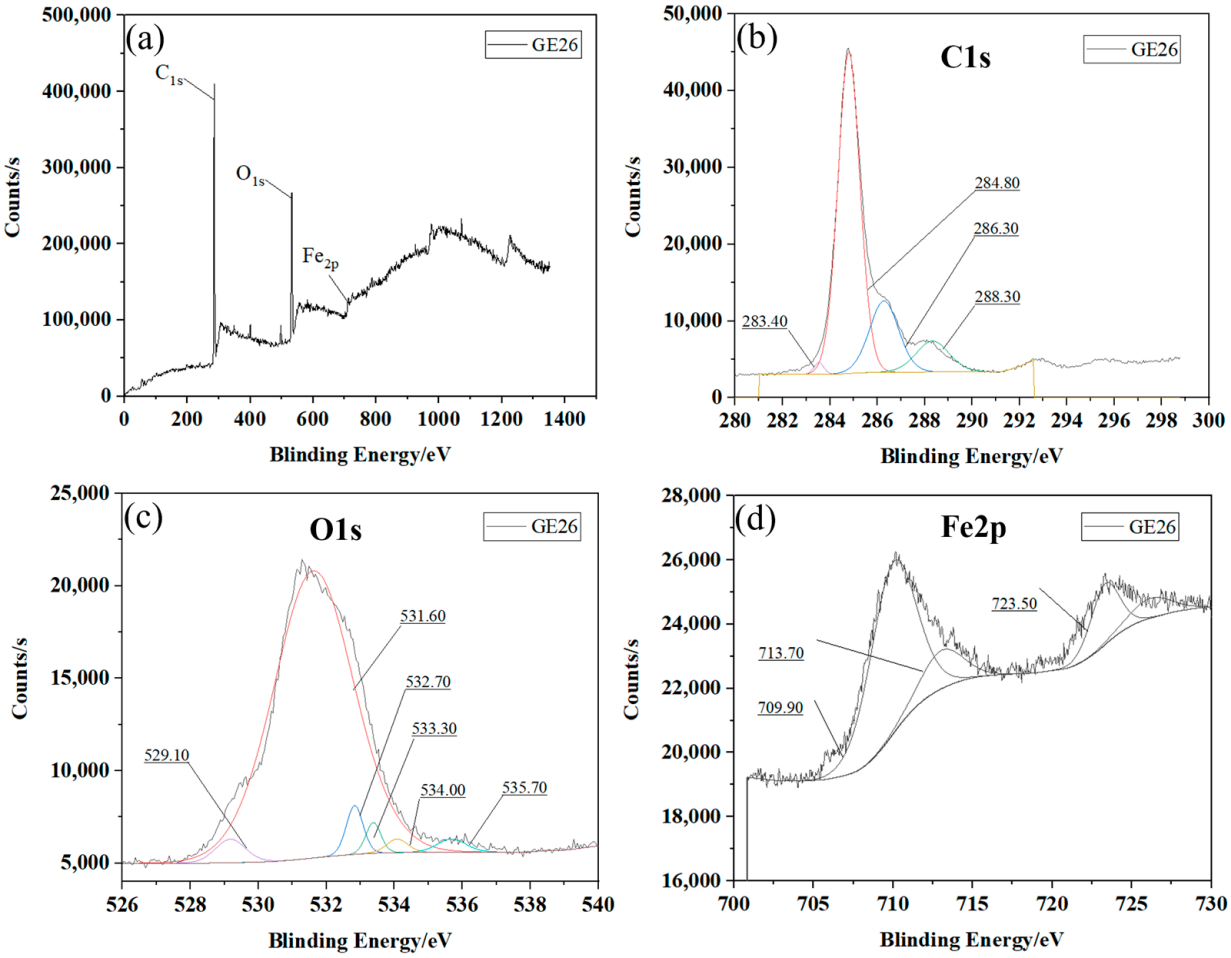


Figure 5. (**a**) XPS binding energy spectrum of the worn surface of the steel ball following the GE aqueous solution test; XPS binding energy spectrum fitting curve of (**b**) C1s, (**c**) O1s and (**d**) Fe2p on the worn surface of the steel ball.

Figure 5c shows the XPS energy spectrum fitting curve for the O1s element on the worn surface of the steel ball. The electron binding energies of oxygen on the steel surface were measured at 529.10 eV, 531.60 eV, 532.70 eV, 533.30 eV, 534.00 eV, and 535.70 eV, corresponding to the molecular structures (–C–O–), $Cr(OH)_3$, Fe_2O_3, Fe_3O_4, and $(–CH_2CH_2O–)_n$, respectively.

Figure 5d displays the XPS energy spectrum fitting curve for the Fe2p element on the worn surface of the steel ball. The electron binding energies of O elements on this surface are 709.9 eV, 713.7 eV, and 723.50 eV, corresponding to the molecular structures Fe_2O_3, FeO and Fe_3O_4. The internal structure of the GE molecule includes (–C–O–) and $(–CH_2CH_2O–)_n$. The formation of $Cr(OH)_3$, Fe_2O_3, FeO and Fe_3O_4 molecules is due to the oxidation reactions of Cr, Fe, and other elements in the steel ball, which form an effective chemical adsorption film on the friction surface during the friction process.

The chemical elements detected on the worn surface were primarily C, O, Fe, and B when using a BA-GE mixed solution as the lubricant (Figure 6a). The electron binding energies of carbon on the worn steel ball surface were 283.81 eV, 284.77 eV, 286.20 eV, and 288.10 eV, corresponding to the molecular structures Cr_3C_2, $(–CH_2CH_2O–)_n$, $–CH_2CH_2–$, C_2H_4, respectively. Cr_3C_2 results from the chemical reaction between the aqueous solution and the steel ball, while $(–CH_2CH_2O–)_n$, $–CH_2CH_2–$ and $–CH=CH_2$ are internal molecular structures of GE (Figure 6b).

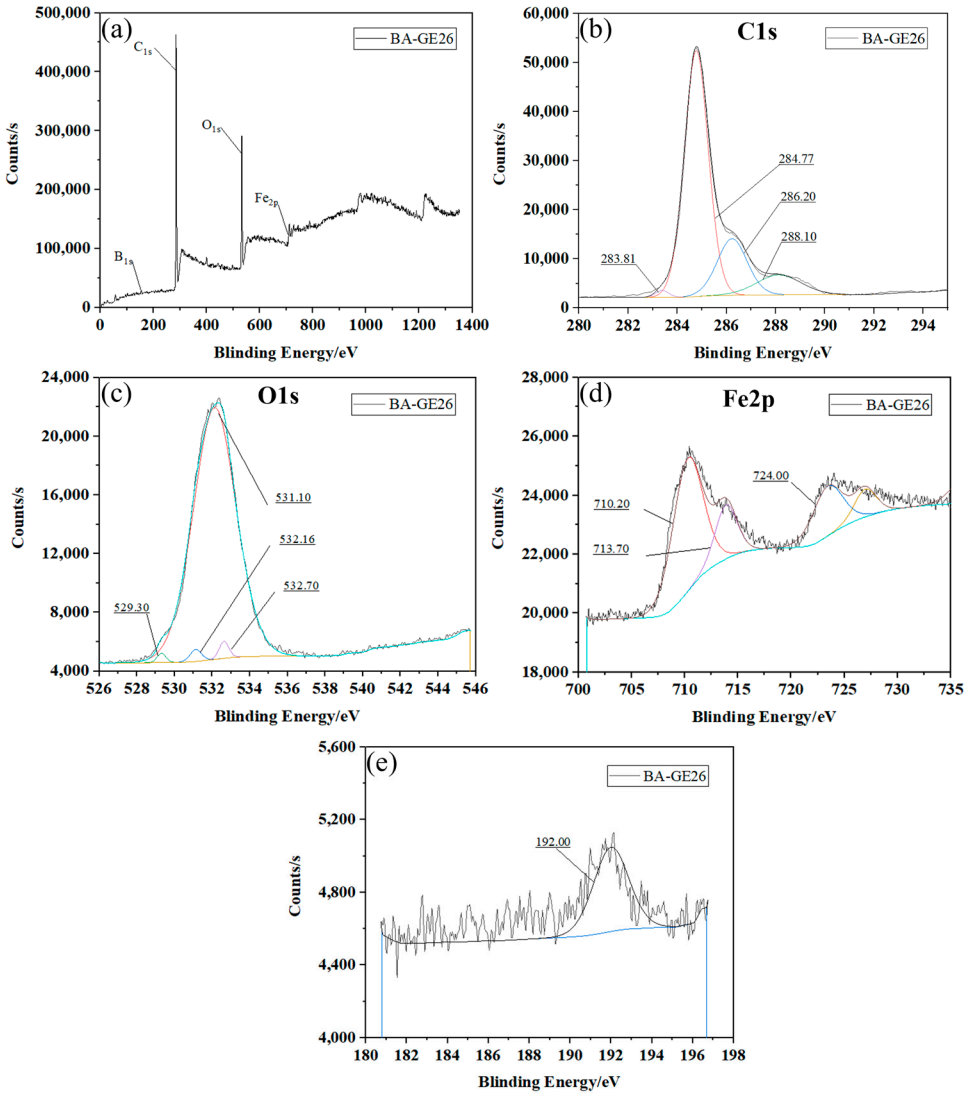


Figure 6. (**a**) XPS binding energy spectrum of BA-GE mixed solution; XPS energy spectrum fitting curves of (**b**) C1s, (**c**) O1s, (**d**) Fe2p and (**e**) B1s on the worn surface of the steel ball.

Figure 6c displays the XPS energy spectrum fitting curve for the O element on the worn surface of the steel ball. The electron binding energies of O are 529.30 eV, 531.10 eV, 532.16 eV, and 532.70 eV, corresponding to the molecular structures Fe_2O_3, CrO_2, B_2O_3 and $(–CH_2CH(OC(O)CH_3)–)_n$, respectively. Fe_2O_3 and CrO_2 result from the oxidation of the steel ball in an aqueous solution, while B_2O_3 forms due to the chemical reaction after adding BA to the GE aqueous solution. The $(–CH2CH(OC(O)CH3)–)_n$ is an internal structural component of the GE molecule. The presence of numerous oxidation products on the worn surface suggests that both mechanical and tribochemical activation under high stress and thermal conditions during sliding contribute to this phenomenon.

Figure 6d displays the XPS energy spectrum fitting curves for Fe elements on the worn surface of the steel ball. The electron binding energies for Fe elements are 710.20 eV, 724.00 eV, and 713.70 eV, corresponding to the molecular structures Fe_2O_3, FeO and Fe_3O_4. This indicates that oxidation occurred on the contact surface during the friction process. No Fe element was detected in the process. Figure 6e shows the XPS energy spectrum fitting curves for B elements on the worn surface. The electron binding energy of 192.00 eV corresponds to B_2O_3. Compared to Figure 6c, adding BA to the GE aqueous solution increases the chemical reaction between the solution and the steel ball's contact surface. Borate ions decompose during friction, allowing B element to enter the friction surface,

significantly reducing friction and wear, and aiding in the formation of a more effective lubrication film.

3.5. Film-Forming Performance

Figure 7 displays the interference patterns indicating the water film thickness for a 50% GE aqueous solution and a BA-50% GE mixture at different linear velocities. The left and right sides of the horizontal interference image represent the entrance and exit of the contact zone, respectively. The horizontal axis delineates the entrance and exits of the contact zone, illustrating how the lubricating water film's thickness varies with linear velocity.

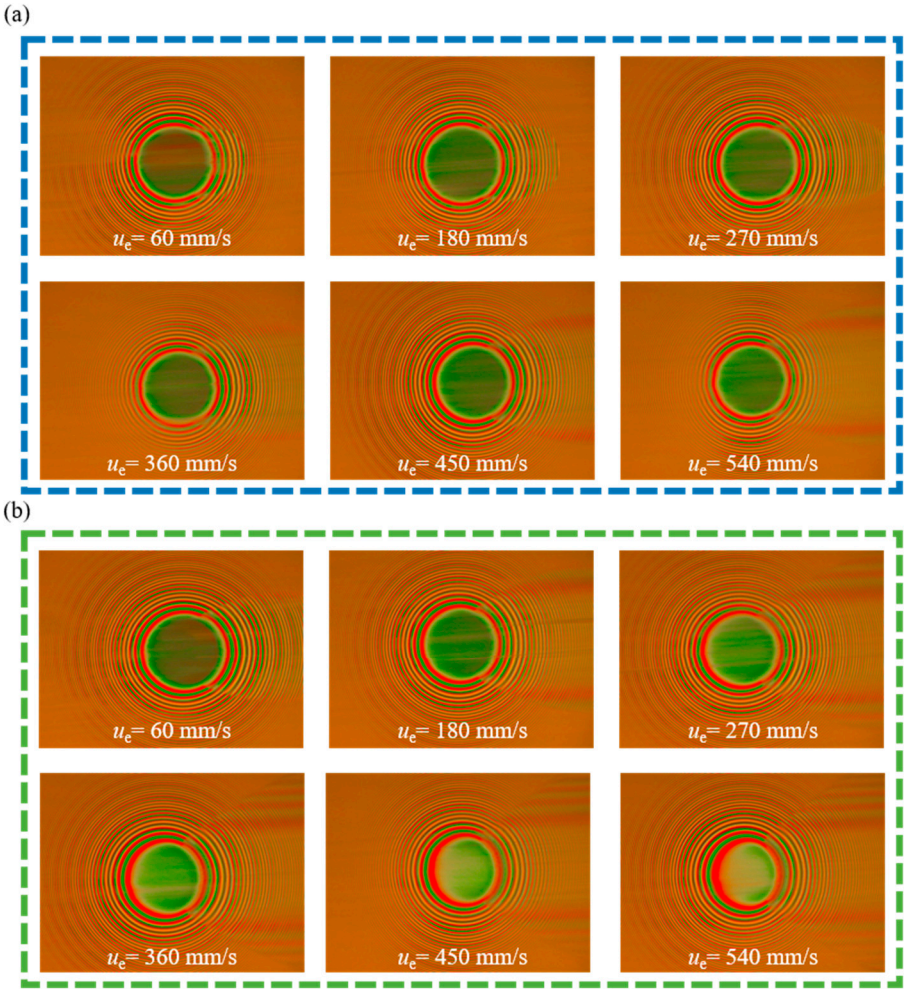


Figure 7. Interference patterns of film thickness of 50%GE (**a**) and BA-10%GE mixed solutions (**b**) at various velocities.

Based on the principle of light interference, changes in the thickness of the lubricating water film are typically associated with the movement of the next order. This was demonstrated using an alternating red-green laser, showing that more orders result in a thicker lubricating water film. The thickness of the film increases significantly with linear speed (Figure 7a).

When the linear velocity reaches 540 mm/s, a 50% GE aqueous solution can form a hydrodynamic pressure effect [35]. At this speed, the water-based lubricant enters the wedge gap between the glass disk and the steel ball, promoting the formation of the lubricating water film. However, for the BA-50%GE mixed solution (Figure 7b), the thickness of the lubricating water film does not increase significantly as the speed rises

from 90 mm/s to 540 mm/s. The hydrodynamic pressure effect of the BA-50%GE mixed solution is weak in this velocity range, leading to minimal change in film thickness [35,36].

While the BA-GE mixture offers benefits such as improved wettability, BA affects the molecular arrangement and interactions within the GE matrix. This influences the fluid's rheological properties relevant to hydrodynamic lubrication. Specifically, BA may interfere with formation of the fluid-dynamic wedge film, which relies on the smooth flow and viscosity characteristics of pure GE. Despite mixtures' advantages in other aspects, this disruption leads to a weaker hydrodynamic effect compared to pure GE.

Figure 8 illustrates the lubricating water film thickness for a 50% GE aqueous solution and a BA-50%GE (1:10) mixed solution at various entrainment velocities. As the entrainment velocity of the 50% GE aqueous solution increases, the water film thickness shows a clear trend of increasing from about 0.014 μm to 0.032 μm. For the BA-50%GE-(1:10) mixed solution, the film thickness also increases with entrainment velocity, but at a faster rate, increasing from 0.016 μm to 0.10 μm. This difference may be due to the higher viscosity of the GE solution, which facilitates the formation of a thicker lubricating film on the metal surface, thereby reducing friction and wear. Additionally, BA may alter the lubrication properties of the GE aqueous solution or influence its surface adsorption behavior, leading to a more rapid increase in water film thickness.

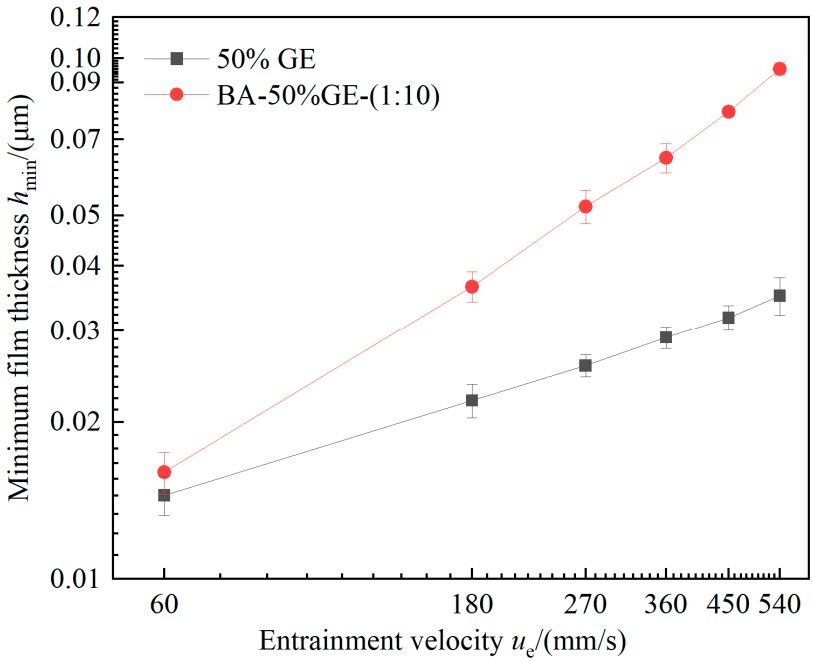


Figure 8. Variations in film thickness for 50%GE and BA-50%GE-(1:10) mixture at different entrainment velocities.

3.6. Extreme Pressure Performance and Anti-Rust Ability

(1) Extreme pressure performance

Figure 9 illustrates the relationship between the wear scar diameter and compensation diameter with 1.05 times for a 50%GE aqueous solution and a BA-50%GE-(1:10) mixed solution under various loads. The wear scar diameter of the BA-50%GE mixed solution is smaller than that of the 50% GE aqueous solution at the same load, indicating that adding BA enhances the anti-friction and anti-wear properties of the GE lubricant. Additionally, the maximum non-seizure load for the 50%GE aqueous solution is 496 N, which increases to 558 N with the addition of BA, resulting in a 12.5% improvement in the extreme pressure performance of the water-based lubricant.

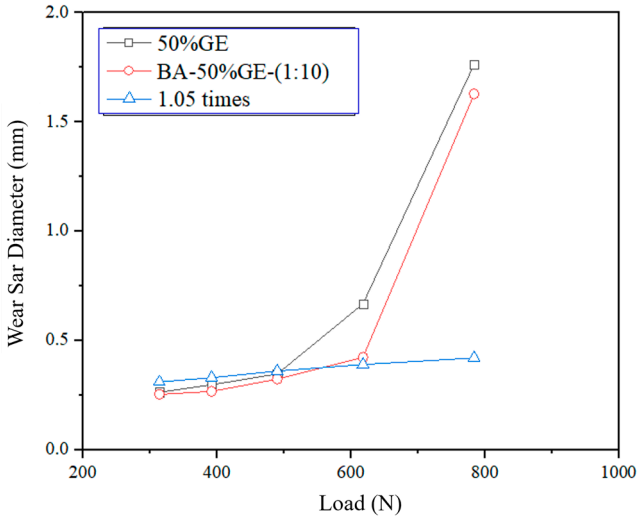


Figure 9. Relationship between measured value of wear scar and compensation diameter with 1.05 times.

(2) Anti-rust ability

Figure 10a–d illustrates the waste liquid changing from dark yellow to lighter as the GE concentration increases. This shift is primarily due to the larger contact area between the steel ball and water and air at low GE concentrations, leading to more Fe_2O_3 during friction [37]. The wear debris from the steel ball contact surfaces causes the solution to appear yellow and turbid after testing. As the GE concentration rises, a lubricating film forms on the contact surface, reducing direct steel ball contact and resulting in a lighter, less turbid waste liquid, indicating improved anti-rust properties of the solution. Figure 10e–h shows the waste liquid from BA-50%GE mixed solutions with varying BA proportions. As BA concentration increases, the solution becomes colorless and transparent, enhancing the anti-rust performance of the GE lubricant.

Figure 10i–l shows that all waste liquids from the BA-50%GE mixed solution remain colorless and transparent as the load increases from 200 N to 500 N. Compared to the waste liquids before adding BA, the mixed solution exhibits more pronounced anti-rust effects, suggesting that chemical reactions during the friction process formed a more stable lubrication film. Figure 10m–p compares the waste liquids from the BA-50%GE mixed solution after experiments at various rotational speeds. The waste liquids have similar colors, but more bubbles form as the speed increases, indicating emulsion precipitation between the base and auxiliary additives. It can be concluded that the mixed solution demonstrates superior anti-rust ability and significantly improved stability at 1000 rpm.

XPS analysis of the worn surface revealed the presence of an adsorbed lubricating water film when using a BA-GE mixed solution as the lubricant. The thickness of this water film increases with higher aqueous viscosity. During rolling and sliding, a lubricating film forms at the entrainment initially, followed by chemical reactions between the additives in the mixed solution and the friction surfaces, enhancing the water film thickness for improved anti-friction and wear resistance. Additionally, the BA-50%GE mixed solution exhibits superior extreme pressure performance and anti-rust capabilities at high speeds of 1000 rpm and heavy loads of 500 N.

Table 1 gives a performance comparison of various water-based lubrication additives. BA-GE significantly surpasses traditional sulfur-phosphorus or ionic liquid s in tribological performance, environmental friendliness, and economic viability. While sulfur-phosphorus lubricant additives have strong extreme pressure properties but moderate anti-friction effects. Nanomaterials in aqueous solutions face dispersion challenges, and ionic liquids are

complex and expensive to prepare. This study adopts the synergistic effects of BA and GE to balance environmental impact, tribological performance, and cost, thereby broadening the application of water-based lubricant additives and offering a viable alternative to traditional high-pollution, high-cost options.

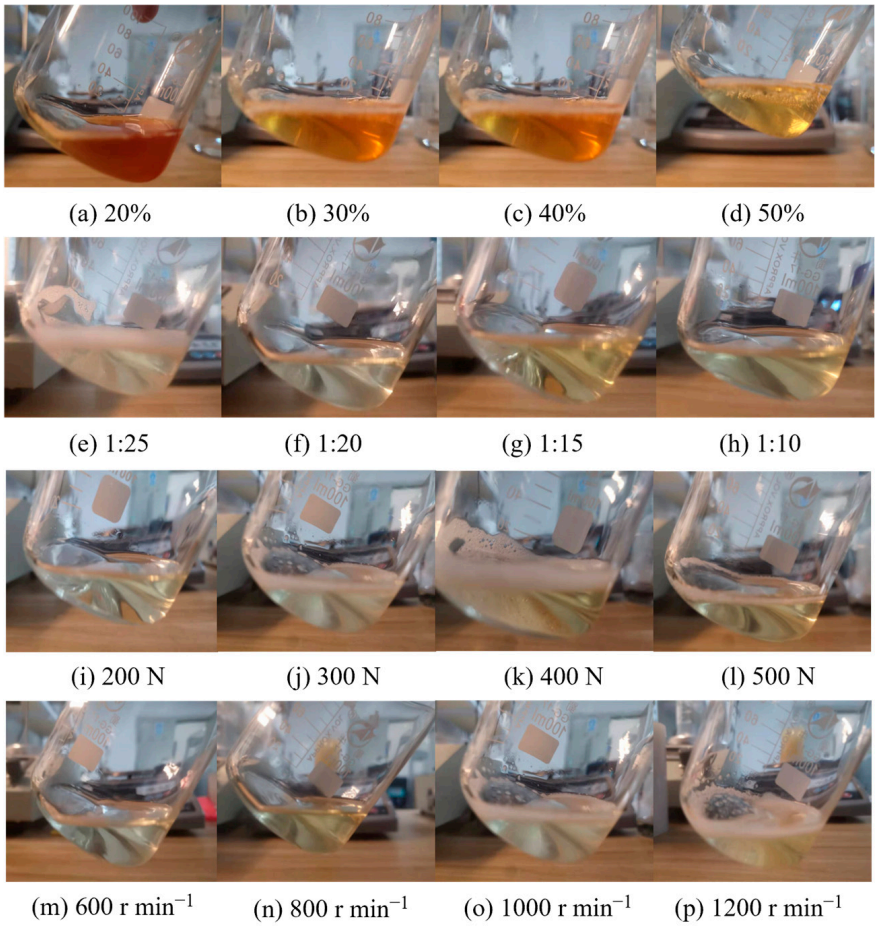


Figure 10. Waste liquid of (**a**–**d**) GE aqueous solution with different concentrations, BA-50%GE mixed solution (**e**–**h**) with different proportions, (**i**–**l**) under different loads and (**m**–**p**) at different rotational speeds after friction experiments.

Table 1. A performance comparison of various water-based lubrication additives.

Type	Additive	Performance	Limitation
Sulfur/phosphorus-based	phosphorus-containing ricinoleic acid (PRA) sulfur-containing ricinoleic acid (SRA) S-P-Cl-containing DEPTP additive	*extreme pressure* (P_B) [38]: water (95 N) with PRA (725 N) with SRA (842 N) *CoF and wear scar diameter* (WSD) (196 N, 1450 r/min) [39]: DEPTP (0.11, 0.8 mm) S-P-Cl-containing (0.084, 0.62 mm)	Harmful to the environment
Boron-based	water-based drilling fluids with borate nanoparticles	*CoF and film strength* [7]: drilling fluids (0.4592, 3881 psi) borate nanoparticles (0.0595, 39,056 psi)	Insufficient high-temperature stability and Poor hydrolysis stability
Nanomaterial-based	polyethylenimine-reduced graphene oxide (PEI-RGO) nanosheets in water	*CoF and WSD* (4 N, 3 Hz) [40]: water (0.491, 182.5 μm) 0.05 wt% PEI-RGO (0.23, 164.2 μm)	Poor dispersion stability and complex preparation process

Table 1. *Cont.*

Type	Additive	Performance	Limitation
Polyether-based	alkyl glyceryl ether with xanthan gum (XG)	*CoF* [11]: water (0.34) with XG (0.06) commercial lubricant DP400 (0.14)	Large addition amount and high cost
Ionic liquid-based	amino acid-based ionic liquids (Lys-DEHP, Arg-DEHP) in water-glycol protic ionic liquid (DE) in water/glycerol and water/PEGsolutions	*CoF*, *and* P_B [41]: W-EG (0.2, 275 N) 1%Lys-DEHP (0.1, 1167 N) 1%Arg-DEHP (0.1, 1118 N) *CoF and WSD* [42]: WGL (0.099, 558 μm) WPEG (0.075, 495 μm) WGL + DE0.5 (n.d.) WPEG + DE0.5 (0.089, 475 μm)	Complex preparation process, high toxicity, and easy to cause corrosion
Our study	BA-50%GE in water	*CoF*, *WSD and* P_B water (0.4, ≥1 mm, n.d.) 50%GE (0.024, 510 μm,496 N) BA-50%GE (0.005, 462 μm, 558 N)	

4. Conclusions

GE and BA serve as water-based lubrication additives to study tribological properties, rheological behavior, film-forming capabilities, and anti-rust performance. The analysis of the molecular structure and chemical bonds indicates that the mixed solution does not form new functional groups but rather exists as a physical mixture. Raising the BA proportion in the mixed solution reduces the contact angle, enhancing the wettability and anti-rust properties of the water-based lubricant. The addition of BA increases the viscosity of the mixed solution, resulting in a thicker lubricating film and improved friction properties. These findings establish both a theoretical and experimental basis for using eco-friendly, water-based lubricants in high-load, high-speed industrial settings.

Author Contributions: Conceptualization, S.H. and Z.H.; methodology, Z.W.; validation, S.H., Z.H. and Z.W.; formal analysis, Z.W.; investigation, S.H.; resources, S.H.; data curation, Z.W.; writing—original draft preparation, S.H.; writing—review and editing, Z.W.; visualization, Z.W.; supervision, Z.H.; project administration, Z.H.; funding acquisition, S.H., Z.H. and Z.W. All authors have read and agreed to the published version of the manuscript.

Funding: This work is financially supported by the Major Science and Technology Project of PetroChina (Grant number 2023ZZ09) and the Tribology Science Fund of the State Key Laboratory of Tribology in Advanced Equipment (Grant number SKLTKF24B20).

Data Availability Statement: The datasets used and/or analyzed during this study are available from the corresponding author upon reasonable request.

Conflicts of Interest: The authors declare no conflicts of interest.

References

1. Rahman, M.H.; Warneke, H.; Webbert, H.; Rodriguez, J.; Austin, E.; Tokunaga, K.; Rajak, D.K.; Menezes, P.L. Water-Based Lubricants: Development, Properties, and Performances. *Lubricants* **2021**, *9*, 73. [CrossRef]
2. Morshed, A.; Wu, H.; Jiang, Z. A Comprehensive Review of Water-Based Nanolubricants. *Lubricants* **2021**, *9*, 89. [CrossRef]
3. Jiang, Z.; Sun, Y.; Liu, B.; Yu, L.; Tong, Y.; Yan, M.; Yang, Z.; Hao, Y.; Shangguan, L.; Zhang, S.; et al. Research progresses of nanomaterials as lubricant additives. *Friction* **2024**, *12*, 1347–1391. [CrossRef]
4. Krim, J.; Smirnov, A.I. Fundamental Mechanisms Underlying the Effectiveness of Nanoparticle Additives to Lubricants: 25 Examples Linking Nano- to Macroscale Friction. *Lubricants* **2024**, *12*, 225. [CrossRef]

5. Jiang, Z.; Wu, J.; Yu, L.; Bi, J.; Wang, Y.; Hu, X.; Zhang, Y.; Li, W. Two-dimensional nanomaterials as lubricant additives: The state-of-the-art and future prospects. *J. Mater. Chem. C* **2025**, *13*, 4327–4373. [CrossRef]
6. Xiong, L.; Lu, H.; Zhong, Q.; He, Z.; Lei, J.; Zhu, X. Tribology Properties of Water-soluble Triazine Derivative Containing Sulfur and Phosphorus on Cemented Carbide. *Lubr. Eng.* **2016**, *41*, 33–37. [CrossRef]
7. Saffari, H.; Soltani, R.; Alaei, M.; Soleymani, M. Tribological properties of water-based drilling fluids with borate nanoparticles as lubricant additives. *J. Pet. Sci. Eng.* **2018**, *171*, 253–259. [CrossRef]
8. Xie, H.; Wei, Y.; Jiang, B.; Tang, C.; Nie, C. Tribological properties of carbon nanotube/SiO_2 combinations as water-based lubricant additives for magnesium alloy. *J. Mater. Res. Technol.* **2021**, *12*, 138–149. [CrossRef]
9. Tang, W.; Jiang, Z.; Wang, B.; Li, Y. Black phosphorus quantum dots: A new-type of water-based high-efficiency lubricant additive. *Friction* **2021**, *9*, 1528–1542. [CrossRef]
10. Yang, D.; Du, X.; Li, W.; Han, Y.; Ma, L.; Fan, M.; Zhou, F.; Liu, W. Facile Preparation and Tribological Properties of Water-Based Naphthalene Dicarboxylate Ionic Liquid Lubricating Additives. *Tribol. Lett.* **2020**, *68*, 84. [CrossRef]
11. De Paula, F.; de Freitas, F.; Nunes, D.; Iglauer, S.; Gramatges, A.; Nascimento, R.; Lachter, E. Alkyl glyceryl ethers as water-based lubricant additives in mixtures with xanthan gum. *Colloids Surf. A Physicochem. Eng. Asp.* **2022**, *634*, 127881. [CrossRef]
12. Liu, W.; Simic, R.; Liu, Y.; Spencer, N. Effect of contact geometry on the friction of acrylamide hydrogels with different surface structures. *Friction* **2022**, *10*, 360–373. [CrossRef]
13. Wang, H.; Zhao, H.; Wu, X.; Zhang, X.; Wang, J.; Liu, Y.; Zhang, J. Superlubricity Achieved by a Transparent Poly(vinylpyrrolidone) Composite Hydrogel with Glycerol Ethoxylate in Ocular Conditions. *Langmuir* **2024**, *40*, 6816–6823. [CrossRef] [PubMed]
14. Meng, F.; Wang, Z.; Chang, Q.; Wang, Z.; Zhang, J.; Geng, X. Tribological Investigation of a Mixed Solution with Superlubricity Achieved. *J. Mech. Eng.* **2022**, *58*, 210–219. [CrossRef]
15. Ge, X.; Li, J.; Zhang, C.; Luo, J. Liquid Superlubricity of Polyethylene Glycol Aqueous Solution Achieved with Boric Acid Additive. *Langmuir* **2018**, *34*, 3578–3587. [CrossRef]
16. Hedayati, H.; Mofidi, A.; Al-Fadhli, A.; Aramesh, M. Solid Lubricants Used in Extreme Conditions Experienced in Machining: A Comprehensive Review of Recent Developments and Applications. *Lubricants* **2024**, *12*, 69. [CrossRef]
17. Zhao, X.; Li, D.; Zhu, H.; Ma, J.; An, Y. Advanced developments in environmentally friendly lubricants for water-based drilling fluid: A review. *RSC Adv.* **2022**, *12*, 22853–22868. [CrossRef]
18. Zakani, B.; Salem, H.; Entezami, S.; Sedaghat, A.; Grecov, D. Effect of particle concentration on lubrication performance of cellulose nanocrystalline (CNC) water-based lubricants: Mixed lubrication regime. *Cellulose* **2022**, *29*, 3963–3984. [CrossRef]
19. Tang, L.; Zhang, Y.; Li, C.; Zhou, Z.; Nie, X.; Chen, Y.; Cao, H.; Liu, B.; Zhang, N.; Said, Z.; et al. Biological Stability of Water-Based Cutting Fluids: Progress and Application. *Chin. J. Mech. Eng.* **2022**, *35*, 3. [CrossRef]
20. Wang, Y.; Guo, Z.; Liu, W. Adhesion behaviors on four special wettable surfaces: Natural sources, mechanisms, fabrications and applications. *Soft Matter* **2021**, *17*, 4895–4928. [CrossRef]
21. Li, Y.; Li, S.; Bai, P.; Jia, W.; Xu, Q.; Meng, Y.; Ma, L.; Tian, Y. Surface wettability effect on aqueous lubrication: Van der Waals and hydration force competition induced adhesive friction. *J. Colloid Interface Sci.* **2021**, *599*, 667–675. [CrossRef]
22. Yu, H.; Chen, H.; Zheng, Z.; Qiao, D.; Feng, D.; Gong, Z.; Dong, G. Effect of functional groups on tribological properties of lubricants and mechanism investigation. *Friction* **2023**, *11*, 911–926. [CrossRef]
23. Yan, L.; Ma, J.; Cui, Z.; Jiang, J.; Song, B.; Pei, X. A New Series of Double-Chain Single-Head Sulfobetaine Surfactants Derived from 1, 3-Dialkyl Glyceryl Ether for Reducing Crude Oil/Water Interfacial Tension. *J. Surfactants Deterg.* **2019**, *22*, 47–60. [CrossRef]
24. Dong, R.; Yu, Q.; Bai, Y.; Wu, Y.; Ma, Z.; Zhang, J.; Zhang, C.; Yu, B.; Zhou, F.; Liu, W.; et al. Towards superior lubricity and anticorrosion performances of proton-type ionic liquids additives for water-based lubricating fluids. *Chem. Eng. J.* **2020**, *383*, 123201. [CrossRef]
25. Li, Y.; Wang, M.; Tan, X.; An, Y.; Liu, H.; Gao, K.; Guo, M. Application of Hybrid Silicate as a Film-Forming Agent in High-Temperature Water-Based Drilling Fluids. *ACS Omega* **2021**, *6*, 20577–20589. [CrossRef]
26. Li, Z.; Chang, Q.; Meng, Y.; Yang, H.; Hao, L. In situ visualization study of tribofilm growth process from magnesium silicate hydroxide nanoparticles. *Tribol. Int.* **2023**, *187*, 108725. [CrossRef]
27. Isernia, L. FTIR Study of the Relation, between Extra-framework Aluminum Species and the Adsorbed Molecular Water, and its Effect on the Acidity in ZSM-5 Steamed Zeolite. *Mater. Res.* **2013**, *16*, 792–802. [CrossRef]
28. White, R.L. A Temperature Perturbation Infrared Spectroscopy Comparison of HY and NaY Zeolite Dehydration/Rehydration. *Minerals* **2024**, *14*, 104. [CrossRef]
29. Ali Al-Mamary, M.; Moussa, Z. Antioxidant Activity: The Presence and Impact of Hydroxyl Groups in Small Molecules of Natural and Synthetic Origin. In *Antioxidants-Benefits, Sources, Mechanisms of Action*; IntechOpen: London, UK, 2021. [CrossRef]
30. Abu-Dief, A.; El-Dabea, T.; El-Khatib, R.; Abdou, A.; Barnawi, I.; Alshehri, H.; Al-Ghamdi, K.; El-Remaily, M. Fabrication, physicochemical characterization and theoretical studies of some new mixed ligands complexes based on N-(1H-benzimidazol-2-yl)-guanidine and 1, 10-phenanthroline: DNA interaction, biological applications and molecular docking approach. *J. Mol. Struct.* **2024**, *1310*, 138328. [CrossRef]

31. Ailincai, D.; Marin, L. Eco-friendly PDLC composites based on chitosan and cholesteryl acetate. *J. Mol. Liq.* **2021**, *321*, 114466. [CrossRef]
32. Bosch, J.; DellaCorte, C. Rheological Characterization and Tribological Evaluation of Water-Based Lubricants in AISI 52100 Bearing Steel. *Tribol. Lett.* **2024**, *72*, 10. [CrossRef]
33. Tu, T.; Wang, W.; Wan, Y.; Pu, J. Tribology Properties of the Aqueous Solution of Polyvinylpyrrolidone. *Mater. Sci.* **2014**, *4*, 103–110. [CrossRef]
34. Zhang, C.; Luo, C.; Ye, L.; Zhang, H.; Xiang, H. Research and Application of Anti-Collapse Lubricant Compound Polyalcohol for Water-Based Drilling Fluid. *Open J. Yangtze Oil Gas* **2021**, *7*, 11–12. [CrossRef]
35. Greenwood, J. Elastohydrodynamic Lubrication. *Lubricants* **2020**, *8*, 51. [CrossRef]
36. Guo, H.; Bao, J.; Zhang, S.; Shi, M. Experimental and Numerical Study on Mixed Lubrication Performance of Journal Bearing Considering Misalignment and Thermal Effect. *Lubricants* **2022**, *10*, 262. [CrossRef]
37. Radhi, N.; Nattah, A.; Al-Khafaji, Z. Identify the effect of Fe_2O_3 nanoparticles on mechanical and microstructural characteristics of aluminum matrix composite produced by powder metallurgy technique. *Open Eng.* **2024**, *14*, 20220519. [CrossRef]
38. Ding, H.; Yang, X.; Xu, L.; Li, M.; Li, S.; Zhang, S.; Xia, J. Analysis and comparison of tribological performance of fatty acid-based lubricant additives with phosphorus and sulfur. *J. Bioresour. Bioprod.* **2020**, *5*, 134–142. [CrossRef]
39. Wang, Y.; Li, N.; Liu, H.; Wang, J.; Han, S. Tribological properties generated by a S-P-Cl-containing additive in water-based lubricant. *Res. Chem. Intermed.* **2021**, *47*, 1615–1623. [CrossRef]
40. Liu, C.; Guo, Y.; Wang, D. PEI-RGO nanosheets as a nanoadditive for enhancing the tribological properties of water-based lubricants. *Tribol. Int.* **2019**, *140*, 105851. [CrossRef]
41. Sun, X.; Liu, X.; Chen, Q.; Guo, P.; Bai, Y.; Zou, K.; Yi, M.; Yang, S.; Cai, M.; Zhou, F.; et al. Amino acid-based ionic liquids as water-ethylene glycol additives towards superior lubricity and corrosion resistance. *J. Mol. Liq.* **2024**, *401*, 124706. [CrossRef]
42. Kreivaitis, R.; Kupčinskas, A.; Gumbytė, M.; Treinytė, J. Tribological properties of bis(2-hydroxyethyl) ammonium oleate in glycerol and polyethylene glycol aqueous solutions. *J. Mol. Liq.* **2023**, *369*, 120933. [CrossRef]

Disclaimer/Publisher's Note: The statements, opinions and data contained in all publications are solely those of the individual author(s) and contributor(s) and not of MDPI and/or the editor(s). MDPI and/or the editor(s) disclaim responsibility for any injury to people or property resulting from any ideas, methods, instructions or products referred to in the content.